Control Engineering Practice 65 (2017) 100–114

Contents lists available at ScienceDirect

Control Engineering Practice

journal homepage: www.elsevier.com/locate/conengprac

Robust control and estimation of clutch-to-clutch shifts

Kirti D. Mishra *, K. Srinivasan

Department of Mechanical and Aerospace Engineering, The Ohio State University, Columbus, OH - 43210, United States

ARTICLE INFO

Keywords:
Clutch-to-clutch
Robust control
Nonlinear estimation
Model-based control

ABSTRACT

Clutch-to-clutch shifts are ubiquitous in automatic transmissions, motivating the need for formal and robust methods for controlling these shifts. Limited sensing in production transmissions poses a severe hurdle for feedback control of these gearshifts. In the current study, nonlinear estimation methods are developed to compensate for limited sensing, and enable model-based closed loop control of the torque and inertia phases of shifts by manipulation of clutch pressures. During the torque phase, the offgoing clutch is controlled to emulate a one-way clutch, which ensures smooth coordination of the two clutches and reduced overall variation in the output shaft torque during the gearshift. During the inertia phase, the oncoming clutch is controlled to ensure smooth engagement at lock-up, resulting in reduction of shock and subsequent driveline oscillations. Controller performance is evaluated through numerical simulation of the proposed observer based controller on an experimentally validated high order model of a stepped production automatic transmission. The results show that shift control objectives were met by the proposed estimation and control strategy in the presence of appreciable model uncertainty and speed sensor noise, thus validating the robustness and practical effectiveness of the controller. Also, the proposed model-based controller was shown to be effective in controlling gearshifts at different power-levels (at different throttle openings), which establishes effectiveness of the same over a wide range of operating conditions.

1. Introduction

A significant majority of production vehicles with automatic transmissions on the road today employ clutch-to-clutch shifts, which involve two actively controlled friction clutches capable of transmitting the load in both slip speed directions; the clutch being released is known as the offgoing clutch, and the clutch being engaged is known as the oncoming clutch. For a typical gearshift, two fundamental specifications need to be met: first, load transfer from the offgoing to the oncoming clutch and second, speed synchronization of the input and output shafts of the transmission after the shift. In a traditional clutch-to-clutch shift, by design, these two specifications are met in two different phases, the former is met in the torque phase, and the latter is met in the inertia phase.

Fig. 1 shows the typical time evolution history of various system variables during a $1-2$ power-on upshift involving only transmission control. At the initiation of the gearshift, following the clutch fill phase, the transmission system enters the torque phase, where the oncoming clutch pressure is ramped-up, transferring the load from the offgoing to the oncoming clutch. This is shown by the decreasing reaction torque at the offgoing clutch during the torque phase. Since the load is transferred from the path of higher gear ratio to one with a lower gear ratio, the torque at the output drops if the turbine torque is relatively unchanged, as is shown by the torque hole in Fig. 1. During this phase, the controller would ideally keep the torque capacity (maximum load that can be carried by a clutch) of the offgoing clutch higher than the reaction torque needed to sustain the motion, and make it zero, i.e. fully release it, exactly when the load carried by the offgoing clutch goes to zero, marking the end of the torque phase and the beginning of the inertia phase. While this occurs naturally in older transmissions equipped with one-way clutches, achievement of the same result by electronic control of the offgoing clutch continues to be a challenge, especially in the absence of feedback signals containing information on the progress of the load transfer. During the inertia phase, the oncoming clutch pressure is further increased or maintained at a high enough level, which increases the output torque, shown as a torque hump in Fig. 1, and the deceleration of the input shaft of the transmission, shown by the decreasing engine speed trace in the same figure. Due to kinematic constraints, the deceleration of the input shaft is reflected in the deceleration of the oncoming clutch slip, which goes to zero resulting in clutch lock-up, at which moment the reaction torque at the

* Corresponding author.
E-mail addresses: mishra.98@osu.edu (K.D. Mishra), srinivasan.3@osu.edu (K. Srinivasan).

http://dx.doi.org/10.1016/j.conengprac.2017.05.007
Received 11 October 2016; Received in revised form 25 May 2017; Accepted 26 May 2017
Available online 22 June 2017
0967-0661/

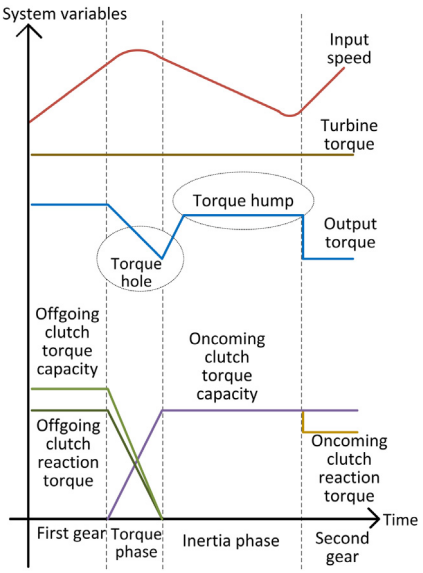

Fig. 1. Typical evolution of system variables during a 1–2 power-on upshift.

oncoming clutch drops below clutch torque capacity marking the end of the gearshift, and the transmission system is in second gear.

Based on the brief introduction to clutch-to-clutch shifts presented above, one can appreciate the need for a torque sensor at the offgoing clutch for the timely release of the same, and smooth coordination between the offgoing and oncoming clutches in the torque phase. Moreover, if it is desired that the oncoming clutch slip speed and the output shaft torque evolve in a controlled fashion, clutch pressures need to be precisely and robustly controlled, motivating the need for closed loop clutch pressure control, which would require clutch pressure sensors. Due to cost and reliability issues, torque and pressure sensors are seldom found in production automatic transmissions, and thus the missing information needs to be estimated online. Such online estimation and controller design should be done carefully, to ensure robust performance of the controller.

Torque phase control is usually accomplished using open-loop techniques, given the small speed change and consequent lack of even minimal sensor information during this phase. Kulkarni, Shim, and Zhang (2007) and Yoon, Khargonekar, and Hebbale (1997) used a model describing the shift dynamics of clutch-to-clutch shifts for offline optimization of clutch pressure trajectories for achieving desired torque response. Closed loop feedback control of the torque phase is rare. Goetz, Levesley, and Crolla (2005) proposed clutch slip control of the offgoing clutch during the torque phase to simulate the operation of a one-way clutch. While this methodology is adequate for preventing clutch tie-up at the end of the torque phase, it is achieved at the expense of additional risk of stick–slip oscillations of the offgoing clutch (Crowther, Zhang, Liu, & Jeyakumaran, 2004).

In the current study, we propose an alternate way to control the offgoing clutch such that it carries load only in one direction and mimics one-way clutch operation, without the potential risk of stick–slip oscillations. Gao, Chen, Li, Tian, and Sanada (2012) developed an observer based controller for the torque phase which, however, suffers from two weaknesses: first, the hydraulic model considered is highly simplified and unrealistic; second, turbine torque is calculated using the torque converter characteristics which again poses robustness issues. We propose accommodation of a realistic model of the hydraulic system, and a novel method to estimate turbine torque in the current study. We also propose a controller structure and implementation that achieves robust control.

Inertia phase control has been traditionally achieved using feedback control techniques, given the availability of speed sensors in production vehicles and appreciable speed change in this phase. In most reported work of this type, the primary approach used for achieving good inertia phase control is to ensure good oncoming clutch slip trajectory tracking. Linear control theory has been used by Gao, Chen, and Sanada (2008), Hojo, Iwatsuki, Oba, and lshikawae (1992), Liu, Gao, and Zheng (2011), Sanada, Gao, Kado, Takamatsu, and Toriya (2012), Sanada and Kitagawa (1998), and Zheng, Srinivasan, and Rizzoni (1999) to achieve desired objectives during the inertia phase. The extensive use of linear control theory can be attributed to a well-developed literature for ensuring robustness against various system uncertainties (Liu et al., 2011; Sanada & Kitagawa, 1998; Sanada et al., 2012). In recent years, nonlinear control theory has been applied to achieve inertia phase control (Gao, Chen, Hu, & Sanada, 2011; Gao, Chen, Sanada, & Hu, 2011; Hu, Tian, Gao, & Chen, 2014), and to extend the effectiveness of model-based control to a wider range of operating conditions. However, in all of these references, a highly simplified shift hydraulic system model was used, which limits the applicability of these works in practice. We propose nonlinear estimation and control approaches that lead to robust inertia phase control. The techniques used here to ensure robust performance of the proposed controller are more general than those used in the authors' own prior publications, and require a more comprehensive approach to estimation. The resulting controller is less conservative than the loop-shaping used by Mishra and Srinivasan (2016) and can accommodate a greater variety of modeling errors as compared to the approach used by Mishra and Srinivasan (2015).

The model of the powertrain used for the simulation, and a corresponding reduced order control-oriented model used for deriving estimation and control algorithms are described in Section 2. The estimation and control algorithms are described in Sections 3 and 4 respectively. Simulation results validating the robustness of the controller are presented in Section 5. Conclusions and directions for future work are discussed in Section 6.

2. Powertrain modeling

The architecture of the powertrain considered for the current study, along with key notation, is shown in Fig. 2, where the main components are the engine, torque converter, transmission mechanical system (or gearbox), transmission hydraulic system, final drive, and drivetrain, represented here by a compliant driveshaft that drives the vehicle inertia equivalently lumped at the wheels. The transmission mechanical system shows only the offgoing and oncoming clutches for a 1–2 upshift, which is a clutch-to-clutch shift and serves as the numerical example to demonstrate the effectiveness of the proposed observer-based controller; the offgoing and oncoming clutches are named LR and ND respectively. A more detailed (stick) diagram of the transmission, containing these two clutches, is shown in Fig. 3. The clutch pressures are generated by the transmission hydraulic system, a schematic of which is shown in Fig. 4.

2.1. Engine model

The engine is modeled as a one degree of freedom system.

$$I_e\dot{\omega}_e = T_i(\omega_e, \alpha) - T_p - T_f - b_e\omega_e \tag{1}$$

where T_i, I_e, ω_e, α, T_f, T_p, and b_e are the engine indicated torque, engine inertia, engine speed, throttle angle, constant component of friction torque, pump torque, and coefficient of viscous friction respectively. The engine indicated torque is modeled as the output of a static map (Barr, 2014), which receives the engine speed and the throttle angle as inputs. For studies involving integrated powertrain control (Bai, Brennan, Dusenberry, Tao, & Zhang, 2010), a richer mean-value model (Cho & Hedrick, 1989) should be used.

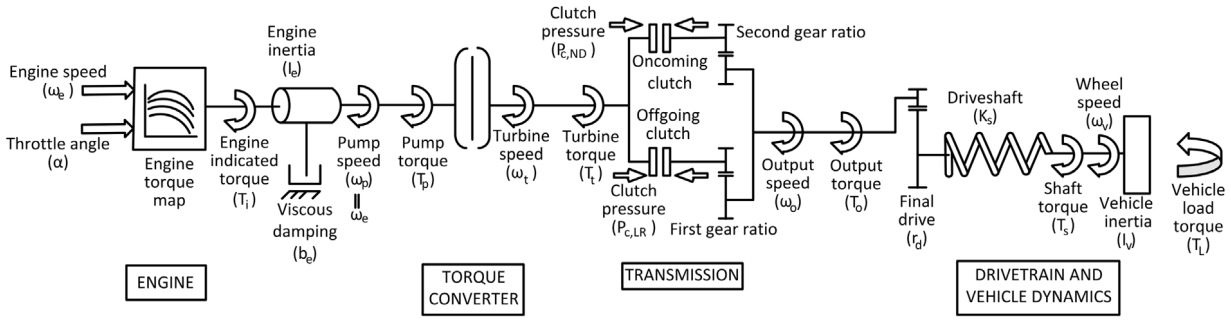

Fig. 2. Powertrain architecture.

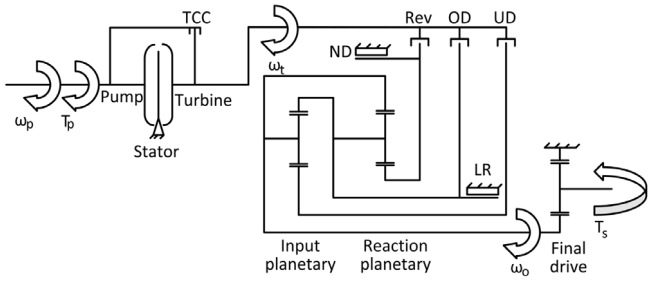

Fig. 3. Stick diagram of transmission system (Watechagit, 2004).

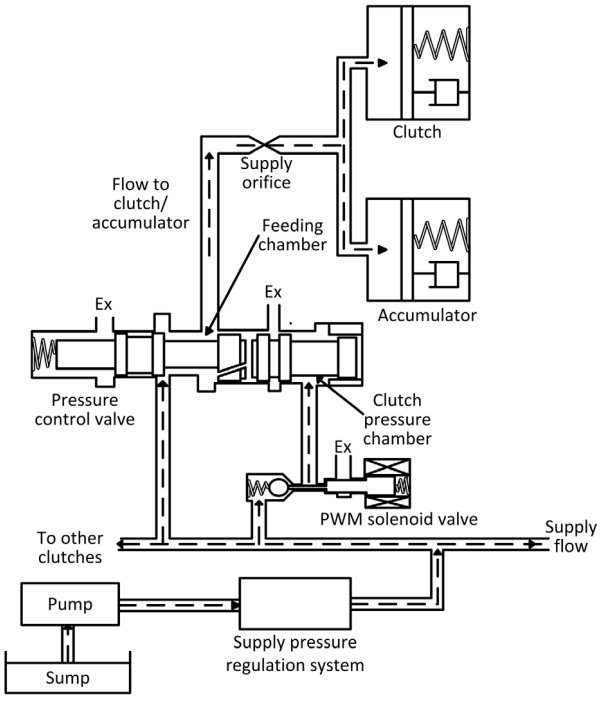

Fig. 4. Simplified schematic of the hydraulic system (Watechagit, 2004).

2.2. Torque converter model

The torque converter plays a critical role in the dynamic performance of automatic transmissions by providing additional damping and torque amplification at lower speeds. Kotwicki's model (Kotwicki, 1982) has been widely used to model torque converters in the literature on control-oriented powertrain modeling. The same model is used here, and is represented by the following equations.
Torque amplification mode ($\omega_t/\omega_p < 0.825$):

$$T_t = a_0\omega_p^2 + a_1\omega_p\omega_t + a_2\omega_t^2$$
$$T_p = b_0\omega_p^2 + b_1\omega_p\omega_t + b_2\omega_t^2. \quad (2)$$

Fluid coupling mode ($\omega_t/\omega_p > 0.825$):

$$T_t = T_p = c_0\omega_p^2 + c_1\omega_p\omega_t + c_2\omega_t^2 \quad (3)$$

T_t, T_p, ω_t, and ω_p denote the turbine torque, pump torque, turbine speed, and pump speed respectively. The constants a_i, b_i, c_i $(i \in \{0,1,2\})$ are known model parameters, and 0.825 denotes the transition speed ratio between the two modes. The transition speed ratio between the two modes depends on the torque converter design and is also believed to depend on operating conditions.

2.3. Clutch model

The transmission system of interest employs wet-type clutches. The torque capacity of a wet clutch, defined as the maximum amount of torque (load) that can be carried by a clutch without slipping, is modeled as a linear function of the clutch pressure.

$$T_c = P_c\mu(\Delta\omega_c)A_cR_c\mathrm{sgn}(\Delta\omega_c) \quad (4)$$

where P_c, A_c, R_c, and $\Delta\omega_c$ represent the clutch pressure, effective pressurized area, effective radius, and clutch slip speed respectively. μ is the clutch friction coefficient and is modeled here by a fourth order polynomial in $\Delta\omega_c$, with h_4 through h_0 being the curve-fit parameters for the data provided by the manufacturer for a new clutch. The curve-fit parameter values would be different for the same clutch and transmission fluid after considerable service.

$$\mu(\Delta\omega_c) = h_4|\Delta\omega_c|^4 + h_3|\Delta\omega_c|^3 + h_2|\Delta\omega_c|^2 + h_1|\Delta\omega_c| + h_0. \quad (5)$$

In (5), h_0 is equal to the static coefficient of friction.

2.4. Transmission model

The transmission system can be divided into two subsystems — mechanical and hydraulic. The mechanical system (gearbox) of the 4-speed production transmission used in the current study consists of a compound gear set (combination of input and reaction planetary gearsets), three friction clutches (Rev, OD, UD), and two band brakes (LR, ND), see Fig. 3. In the current study, a power-on 1–2 upshift is used to validate the proposed observer-based controller, which for the transmission system of interest is a clutch-to-clutch shift in the LR and ND brakes in the roles of the offgoing and oncoming clutches respectively. It should be noted that 1–2 upshifts are typically more difficult to control among upshifts, due to the larger gear ratio change involved. The transmission hydraulic system consists of a central pump, a pressure regulation system to keep the supply (line) pressure constant by using mechanical feedback and, for each clutch, a PWM solenoid

valve, a pressure control valve (PCV), a supply side orifice and a clutch–accumulator combination, see Fig. 4. All the parameters associated with the transmission model are taken from Watechagit (2004).

2.4.1. Transmission mechanical model

As indicated earlier, a typical power-on clutch-to-clutch upshift starts with the transfer of load from the offgoing to the oncoming clutch. This is achieved through reduction of the offgoing clutch pressure and increase of the oncoming clutch pressure. In this phase, the torque phase, the offgoing clutch does not slip and the transmission mechanical system has just one degree of freedom in the form of the oncoming clutch slip speed ω_{sr}, where sr denotes the sun gear of the reaction planetary gearset. The defining equation and parameters are

$$\begin{aligned}&\dot{\omega}_{sr} = \kappa_1 T_s + \kappa_2 T_t + \kappa_3 \mu(\omega_{sr}) P_{c,ND}\\ &\kappa_1 = \frac{-p_{11} r_d}{I_{eq,1}},\ \kappa_2 = \frac{p_{21}}{I_{eq,1}},\ \kappa_3 = \frac{-A_c R_c \text{sgn}(\omega_{sr})}{I_{eq,1}}\\ &I_{eq,1} = I_{sr} + I_{rr} p_{11}^2 + p_{21}^2 (I_t + I_{si})\end{aligned} \tag{6}$$

where T_s, T_t, and $P_{c,ND}$ represent the output shaft torque (after the final drive), turbine torque and oncoming clutch pressure respectively. The constants p_{ij}, $i,j \in \{1,2\}$, are derived from lever diagram of the compound planetary gearset, r_d denotes the final drive ratio, and $I_t, I_{sr}, I_{rr}, I_{si}$ represent lumped inertias at the torque converter turbine side, sun gear of the reaction planetary gearset, ring gear of the reaction planetary gearset, and sun gear of the input planetary gearset respectively. The planetary gear set model used here takes only inertial effects into account and ignores gear friction as well as gear tooth stiffness, the latter being significant primarily for noise and vibration studies. The reaction torque at the offgoing clutch (RT_{LR}), during the torque phase, and the parameter definitions are given by

$$\begin{aligned}&RT_{LR} = \alpha_1 T_s + \alpha_2 T_t + \alpha_3 \mu(\omega_{sr}) P_{c,ND}\\ &\alpha_1 = -p_{12} r_d - I_{eq,2}\kappa_1,\ \alpha_2 = p_{22} - I_{eq,2}\kappa_2\\ &\alpha_3 = -I_{eq,2}\kappa_3,\ I_{eq,2} = p_{11} p_{12} I_{rr} + p_{22} p_{21} (I_t + I_{si}).\end{aligned} \tag{7}$$

When the load on the offgoing clutch equals the clutch torque capacity, the offgoing clutch begins to slip marking the end of the torque phase, following which the clutch-to-clutch shift enters the inertia phase. Ideally, this should happen when the offgoing clutch torque goes to zero.

During the inertia phase, both the offgoing and oncoming clutches slip, and the transmission mechanical system is described as follows,

$$\begin{bmatrix}\dot{\omega}_{sr}\\ \dot{\omega}_{cr}\end{bmatrix} = \begin{bmatrix}q_1 & q_2 & q_3\mu(\omega_{sr}) & q_4\mu(\omega_{cr})\\ p_1 & p_2 & p_3\mu(\omega_{sr}) & p_4\mu(\omega_{cr})\end{bmatrix}\begin{bmatrix}T_s\\ T_t\\ P_{c,ND}\\ P_{c,LR}\end{bmatrix}$$

$$\begin{aligned}&q_1 = -(p_{12}\varphi_1 + p_{11}\varphi_2) r_d,\ q_2 = (p_{22}\varphi_1 + p_{21}\varphi_2)\\ &q_3 = -\varphi_2 A_c R_c \text{sgn}(\omega_{sr}),\ q_4 = -\varphi_1 A_c R_c \text{sgn}(\omega_{cr})\\ &p_1 = -(p_{12}\varphi_3 + p_{11}\varphi_4) r_d,\ p_2 = (p_{22}\varphi_3 + p_{21}\varphi_4)\\ &p_3 = -\varphi_4 A_c R_c \text{sgn}(\omega_{sr}),\ p_4 = -\varphi_3 A_c R_c \text{sgn}(\omega_{cr})\\ &\varphi_1 = \frac{1}{\Delta}(p_{11} p_{12} I_{rr} + p_{21} p_{22} (I_t + I_{si})) = \varphi_4\\ &\varphi_2 = -\frac{1}{\Delta}(I_{cr} + p_{12} p_{22} I_{rr} + p_{22}^2 (I_t + I_{si}))\\ &\varphi_3 = \frac{1}{\Delta}(I_{sr} + p_{11}^2 I_{rr} + p_{21}^2 (I_t + I_{si}))\\ &\Delta = (p_{12} p_{11} I_{rr} + p_{22} p_{21} (I_t + I_{si}))^2 - (I_{sr} + p_{11}^2 I_{rr}\\ &\quad + p_{21}^2 (I_t + I_{si}))(I_{cr} + p_{12} p_{22} I_{rr} + p_{22}^2 (I_t + I_{si}))\end{aligned} \tag{8}$$

where ω_{cr} denotes the slip speed at the carrier gear of the reaction planetary gearset, which is the offgoing clutch slip speed, I_{cr} represents inertia lumped at the carrier gear of the reaction planetary gearset, and $P_{c,LR}$ represents the offgoing clutch pressure. If $P_{c,LR}$ is not zero at the end of the torque phase, the two clutches are in conflict (clutch tie-up) resulting in a further lowering of the output shaft torque until $P_{c,LR}$ becomes zero. The oncoming clutch pressure $P_{c,ND}$ is raised to decelerate the input shaft of the transmission during the inertia phase. The clutch pressures are generated by the transmission hydraulic system, which is described next.

2.4.2. Transmission hydraulic model

The transmission hydraulic system in this case consists of an electro-hydraulic actuation system for each clutch and a central line pressure regulation system. The schematic for the transmission hydraulic system is shown in Fig. 4. Detailed modeling of shift hydraulic system for the production transmission of interest here has been performed by Watechagit (2004), where a high fidelity 13^{th} order model was derived using Newtonian dynamics and subsequently reduced to 5^{th} order using energy analysis techniques (Louca, Stein, Hulbert, & Sprague, 1997). Both of these models were experimentally validated in the same work (Watechagit & Srinivasan, 2003).

This fifth order model is chosen as the starting point for the current study, and needs to be simplified further to accommodate model-based controller design. In order to simplify the model further, it is assumed that the line pressure of the hydraulic system is approximately constant. Simulation results of the full (13^{th}) order model indicate that line pressure fluctuates about an approximately constant mean value and at a frequency equal to that of PWM solenoid valve (64 Hz). Since these fluctuations are attenuated by the accumulator dynamics, we consider it reasonable to neglect the line pressure dynamics. Consequently, we use here a third order model representation of the shift-hydraulic system dynamics for each clutch. It is noted here that the assumption of constant line pressure offers an additional advantage in that it decouples the shift hydraulic models for different clutches, leading to a simplified process of controller design.

The three main energy storage elements in the reduced model are associated with the magnetic flux (ϕ), the pressure control valve (PCV) piston position (x_{pcv}), and the accumulator position (x_a). In response to the duty cycle commanded by the controller, a voltage is generated by the PWM circuit. This voltage energizes the solenoid and leads to the production of magnetic flux, which results in a force on the plunger, and in turn causes the solenoid valve to open and close at the same frequency as the PWM voltage. Corresponding to the opening and closing of the valve, fluid in-flows and exhaust-flows are generated, which exert pressure on the spool of the PCV, and its resulting motion (x_{pcv}). The opening and closing of the PCV gives rise to the flow to (inflow phase), and from (exhaust phase), the clutch–accumulator chamber respectively. This flow determines the motion of the accumulator piston. It was shown by Watechagit (2004) that, following the clutch filling phase, clutch dynamics and various friction forces are negligible. The motion of the accumulator piston (x_a) and its relationship with clutch pressure is described below.

$$\begin{aligned}&\dot{x}_a = \begin{cases}\dfrac{1}{A_a}\left(C_d A_{incE}\sqrt{\dfrac{2(P_s - P_c)}{\rho}}\right), & \text{Inflow phase}\\ \dfrac{1}{A_a}\left(C_d A_{excE}\sqrt{\dfrac{2P_c}{\rho}}\right), & \text{Exhaust phase}\end{cases}\\ &P_c A_a = K_a x_a\end{aligned} \tag{9}$$

where A_a is the accumulator piston area, K_a represents the accumulator spring constant, and A_{incE}, and A_{excE} represent the effective supply orifice areas for the inflow and exhaust phases respectively.

$$\begin{aligned}A_{incE} &= \frac{A_{in}(x_{pcv}) A_{inc}}{\sqrt{A_{in}(x_{pcv})^2 + A_{inc}^2}}\\ A_{excE} &= \frac{A_{ex}(x_{pcv}) A_{inc}}{\sqrt{A_{ex}(x_{pcv})^2 + A_{inc}^2}},\end{aligned} \tag{10}$$

where A_{inc} is the area of the supply-side orifice, and A_{in}, A_{ex} are the inflow (supply) and exhaust port areas of the PCV respectively. They are expressed by the following equations, where x_{in}, x_{out} are the displacements of the PCV spool corresponding to the opening of the supply port and the closing of the exhaust port respectively. d_{sp1}, d_{sp2} are

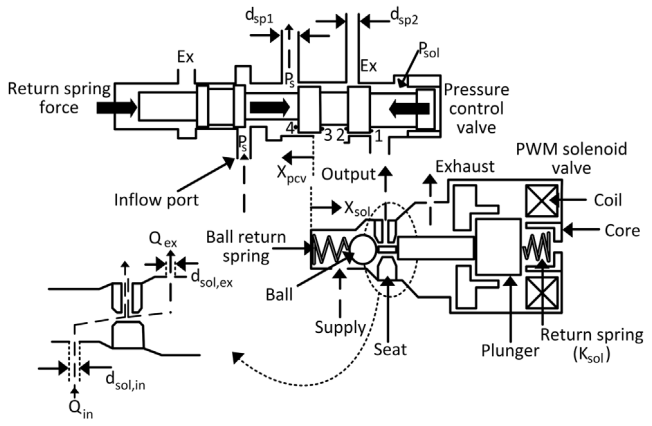

Fig. 5. PCV and solenoid valve in inflow phase (Watechagit, 2004).

the diameters of valve lands at the supply and exhaust ports respectively, see Fig. 5.

$$\begin{aligned} A_{in}(x_{pcv}) &= (x_{pcv} - x_{in})\pi d_{sp1} \\ A_{ex}(x_{pcv}) &= (x_{out} - x_{pcv})\pi d_{sp2}. \end{aligned} \tag{11}$$

2.5. Transmission hydraulic system model order reduction and experimental validation

The third order transmission hydraulic system model presented in the preceding subsection is highly nonlinear and not conducive to model-based controller design. In order to simplify the model further, the dominant (slower) dynamics of the transmission hydraulic model will be recognized and retained, while the faster dynamical states will be eliminated. In conjunction with this, the method of state-space averaging will be employed to arrive at a first order nonlinear model of the transmission hydraulic system. The method of state-space averaging is not used to reduce the order of the model per se, but only in redefining the control input so that the state equations of the reduced order model are affine (or linear) in the newly defined input.

Electrohydraulic systems usually have dynamic characteristics which may enable further model order reduction by exploiting large differences in the time scales of the transients associated with the dynamic states of the systems. For the third order model presented above, it is reasonable to expect that the dominant dynamics would involve the accumulator piston position (or the related accumulator/clutch pressure). This is because accumulators are designed to store and release energy in a controlled manner that would result in good shift quality. The above expectation is in fact borne out for the given transmission of interest. The accumulator piston position (which is linearly related to the clutch pressure, see (9)) was found to be dominant over the other two states (magnetic flux and PCV piston position) from simulation of the experimentally validated 13^{th} order model.

Based on these observations, the dynamics of the magnetic flux and spool position of PCV are neglected for controller design. Doing so, a first order nonlinear model for the shift hydraulic system is obtained, which is given by (9), (10), and (11), where x_{pcv} is an intermediate input that needs to be expressed in terms of the actual control input γ, the commanded duty cycle to the solenoid valve. The usual process for such an identification entails the generation of a look-up table, based on a set of steady state tests, that relates the input γ to the variable x_{pcv}. It should be noted that due to the nature of PWM excitation, the PCV spool valve position x_{pcv} never attains a steady state value but oscillates around a mean value that is determined by γ. Thus the process of look-up table identification is not very straight forward, although one can construct a steady-state map relating the mean value of x_{pcv} and the corresponding duty cycle γ. Also, the intermediate input x_{pcv} enters the model in a non-affine manner, which makes the process of controller design challenging. Affine systems are systems where the control input enters the system state equations linearly, though the equations may be nonlinear in state variables. In order to avoid having to deal with the oscillating nature of x_{pcv} and simultaneously transform the model represented by (9), (10), and (11) into the affine form, the method of state space averaging is used. This method has been used for pneumatic PWM control systems (Shen, Zhang, Barth, & Goldfarb, 2005), but has not been applied to a hydraulic PWM system.

The method of state-space averaging is presented next. Let $u = 0$ and $u = 1$ denote the inflow phase (PWM valve fully open) and exhaust phase (PWM valve fully closed) respectively. For the valve in the fully open state, the effective supply orifice area A_{incE} attains its maximum value $A_{incE,m}$, and for the valve in the fully closed state A_{excE} attains its maximum value $A_{excE,m}$. For notational convenience, define:

$$\begin{aligned} f^+ &:= \frac{1}{A_a}\left(C_d A_{incE,m}\sqrt{\frac{2(P_s - P_c)}{\rho}}\right) \\ f^- &:= -\frac{1}{A_a}\left(C_d A_{excE,m}\sqrt{\frac{2P_c}{\rho}}\right). \end{aligned} \tag{12}$$

In addition, let ΔT denote the time period of the PWM valve, and γ be the commanded duty cycle. By definition, the valve remains open and closed for $\gamma\Delta T$ and $(1-\gamma)\Delta T$ time durations respectively. Now, by using (9) and (12), the dynamic equations of the hydraulic system, averaged over the time period ΔT of the PWM solenoid valve, are given below.

$$\begin{aligned} \dot{x}_{a,avg} &= \frac{f^+\gamma\Delta T + f^-(1-\gamma)\Delta T}{\Delta T} \\ &= f^+\gamma + f^-(1-\gamma) \\ P_{c,avg}A_a &= K_a x_{a,avg}. \end{aligned} \tag{13}$$

Notice that the intermediate input x_{pcv} has disappeared from the averaged dynamics equation, and the control input γ appears linearly. It is hypothesized here that a simplified model representation similar to (13) can be derived for any shift hydraulic system having a dominant pressure controlling element, like the accumulator in the transmission of interest, which is relatively slower than the other components of the shift hydraulic system.

The responses of the third order model used in the current study to represent hydraulic system dynamics, and of the first order model obtained with state space averaging, are compared in Fig. 6 with experimentally measured clutch pressure responses from vehicle tests (Watechagit & Srinivasan, 2003). As mentioned earlier, the ND clutch is the oncoming clutch for the 1–2 upshift. Fig. 6 shows the ND clutch response during disengagement (top) and engagement (bottom) for the state-space averaged first order model, the third order nonlinear model from which the first order model is derived, and physical system. One can note that the response of the third-order nonlinear model is closer to the experimental data than that of the first order model, as expected; however, the response of the latter is sufficiently close to the experimental data for the purpose of model-based controller design. In Section 4.4, appropriate measures will be taken to incorporate robustness in the controller against such errors in the model used to derive the controller.

2.6. Vehicle dynamics and driveline model

The vehicle dynamics model used here represents only the longitudinal dynamics of the vehicle, which has been found to be sufficient for the evaluation of transmission controller performance (Cho & Hedrick, 1989; Zheng et al., 1999). The torque produced at the output shaft of the transmission system propagates through the driveline (final drive, shafts, couplings, etc.) to drive the vehicle. The driveline torsional characteristics are represented by a single compliant shaft, drivetrain

compliance being the dominant dynamic characteristic at the low frequencies of interest for shift quality control. The resulting vehicle dynamics model is expressed as,

$$\begin{aligned}\dot{T}_s &= K_s(\omega_o - \omega_v)\\ \dot{\omega}_v &= \frac{1}{I_v}(T_s - T_L)\end{aligned} \tag{14}$$

where $K_s, \omega_o, \omega_v, I_v$ denote the lumped driveline compliance, final drive output shaft speed, wheel speed, and effective inertia of the vehicle lumped at the wheel, respectively. T_L is the load torque on the wheel, which is a measure of vehicle road load and is modeled as,

$$T_L = r(f_1 + f_2 r^2 \omega_v^2) \tag{15}$$

where r is the wheel's radius and f_1, f_2 are known constants. This model of vehicle longitudinal dynamics does not accommodate tire longitudinal slip, and is more appropriate for conditions involving low longitudinal slip. Inclusion of such longitudinal slip is straightforward (Zheng et al., 1999). Given the focus of the current work on modeling and control of transmission shift quality, it is of secondary importance.

3. Estimator design

The controller to be described in Section 4 requires information about the output shaft torque (T_s), turbine torque (T_t), oncoming clutch pressure ($P_{c,ND}$), and reaction torque at the offgoing clutch (RT_{LR}) during the torque phase. Transmission systems, in general, are sensor-poor and the ones in production are not equipped with torque sensors due to their high cost and low durability. In addition to this, planetary automatic transmissions usually do not come with any clutch pressure sensors because of the large number of clutches and the cost and reliability consequences of instrumenting all of the clutches. However, dual clutch transmissions come equipped with clutch pressure sensors as there are only two clutches, which eliminates the need for clutch pressure estimation.

We present scenarios for estimating all of the required variables, including cases where clutch pressure sensors are unavailable. Shaft torque is estimated using a Luenberger observer, with gains selected to ensure robustness against parametric uncertainty. Reaction torque at the offgoing clutch need only be estimated for the torque phase alone, since the offgoing clutch is fully released during the inertia phase. The turbine torque and oncoming clutch pressures are estimated differently for the torque and inertia phases due to the differences in the governing differential equations for the two phases.

Model-based estimation and control of engine and vehicle dynamics is more established than similar approaches for transmission systems. Also, chassis and engine control systems are richer with respect to the level of sensing and on-line estimation available as compared to transmission systems. We note that sensory and estimation information from engines and chassis subsystems can be used to facilitate the development of algorithms for estimating operating variables in the transmission subsystem. More specifically, the load torque on the vehicle and the indicated torque of the engine will be assumed to be known quantities in the following discussion, due to the availability of well-developed and validated estimation algorithms for these operating variables.

3.1. Shaft torque observer design

A Luenberger observer was used to estimate the shaft torque (T_s) based on the vehicle dynamics and transmission driveline models of the powertrain given by (14), which can be written in state space form,

$$\begin{aligned}\begin{bmatrix}\dot{T}_s\\ \dot{\omega}_v\end{bmatrix} &= \begin{bmatrix}0 & -K_s\\ \frac{1}{I_v} & 0\end{bmatrix}\begin{bmatrix}T_s\\ \omega_v\end{bmatrix} + \begin{bmatrix}K_s & 0\\ 0 & -\frac{1}{I_v}\end{bmatrix}\begin{bmatrix}\omega_o\\ T_L\end{bmatrix}\\ y &= \begin{bmatrix}0 & 1\end{bmatrix}\begin{bmatrix}T_s\\ \omega_v\end{bmatrix}\end{aligned} \tag{16}$$

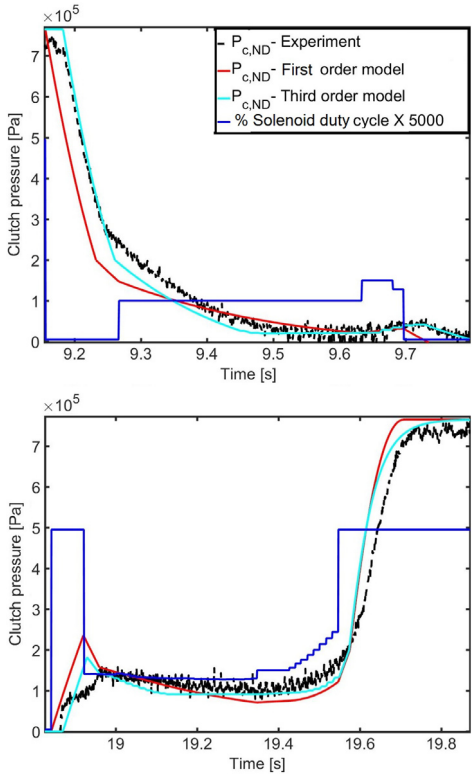

Fig. 6. Comparison of responses of third-order and first-order models with experiment, for ND Clutch during disengagement (top) and engagement (bottom).

where ω_o, T_L are the known inputs and y is the measured output, wheel speed. Due to the availability of speed sensors, ω_o is known by measurement. T_L is either known through (15) or estimated by some other means, as shown by Azzoni, Moro, Ponti, and Rizzoni (1998) and Pavkovi, Deur, Kolmanovsky, and Hrovat (2008). It should be noted that in these and other studies, the load torque on the vehicle is estimated when the transmission is in fixed gear and not during a gearshift. However, since the load torque on the vehicle depends on the vehicle-environment interaction, which does not change instantaneously, the estimate of load torque just before the gearshift serves as a reasonable estimate of the same during the gearshift, as is discussed by Vahidi, Stefanopoulou, and Peng (2005). Either of the methods for load torque estimation, through use of (15) or by online estimation techniques, results in some uncertainty in the estimated load torque, requiring appropriate robustness of the proposed observer-based controller. Now let

$$\mathbf{x} := \begin{bmatrix}T_s\\ \omega_v\end{bmatrix},\ A := \begin{bmatrix}0 & -K_s\\ \frac{1}{I_v} & 0\end{bmatrix},\ B := \begin{bmatrix}K_s & 0\\ 0 & -\frac{1}{I_v}\end{bmatrix}$$
$$C = \begin{bmatrix}0 & 1\end{bmatrix},\ \mathbf{u} := \begin{bmatrix}\omega_o\\ T_L\end{bmatrix}. \tag{17}$$

The Luenberger observer is given by,

$$\dot{\hat{\mathbf{x}}} = A\hat{\mathbf{x}} + B\mathbf{u} + L(y - \hat{y}),\quad L := \begin{bmatrix}l_1 & l_2\end{bmatrix}^T \tag{18}$$

where $\hat{\mathbf{x}}$ denotes the estimate of $\mathbf{x}$. The column vector L denotes the observer gain. Since the pair (C, A) is observable, eigenvalues of the closed loop system characterized by the matrix $A - LC$ can be placed arbitrarily to make the characteristic polynomial Hurwitz, leading to asymptotic convergence of the estimation error to zero.

Criteria in addition to asymptotic convergence of the estimation error may be emphasized in choosing the gain matrix L. In the current study, L was chosen to ensure robustness against uncertainty in the

lumped driveline stiffness K_s, which usually is not known very accurately. If the uncertainty in the lumped compliance is denoted by ΔK_s, then the following can be easily derived.

$$\tilde{T}_s(s) = \frac{s + l_2}{s^2 + l_2 s + \frac{l_1 + K_s}{I_v}} \Delta K_s(\omega_o - \omega_v)(s) \tag{19}$$

where $\tilde{T}_s$ denotes the estimation error of the output shaft torque. Since ΔK_s, ω_o, and ω_v do not change substantially during the shift as its duration is short, it is reasonable to assume $\Delta K_s(\omega_o - \omega_v)$ to be a low frequency signal. Thus l_1, l_2 were selected to shape the frequency response of the transfer function in Eq. (19) to reject low frequency disturbances as well as the high frequency sensor noise which might be present in the measured rotational speeds. In the current study, speed sensor signals are modeled to be noisy, as will be seen in Section 5. More precisely, the gains l_1, l_2 are tuned under the assumption that the uncertainty in the lumped driveline compliance K_s could be as high as 30%.

3.2. Torque phase observer design

Kotwicki's static model (Kotwicki, 1982) for torque converters is usually considered to be sufficiently accurate for transmission shift controller design, for example, see Gao et al. (2012). However, it should be noted that Kotwicki's model does not take into account variations in temperature of the torque converter oil, fluid inertia, etc., and hence open loop estimation of turbine torque based on Kotwicki's model is questionable for control and diagnosis purposes. This motivates the need for online closed loop estimation of the turbine torque.

We begin by noting that, just before the start of the torque phase, the torque converter can either be locked by the torque converter clutch, or be in the fluid coupling or torque amplification mode. We assume here that the torque converter mode remains unchanged during the torque phase since speeds do not change substantially during this phase, the assumption being supported by the simulation results shown later. In the torque-amplification mode, the turbine torque depends significantly upon torque converter characteristics in addition to the pump torque, and hence its estimation requires significant information from the transmission side. However, during the torque phase, the transmission system just has one degree of freedom (see (6)), implying that simultaneous estimation of the turbine torque and oncoming clutch pressure is not possible without additional information. For the remaining two cases, a locked torque converter clutch or a torque converter in the fluid coupling mode, the transmission system is coupled to the engine and thus information from the engine side can be used to estimate the turbine torque, allowing independent estimation of the oncoming clutch pressure from (6).

In the current study, we assume that the torque converter is either locked or in the fluid coupling phase. If neither is the case, we would need to use Kotwicki's model of the torque converter to estimate turbine torque. The assumption is a reasonable one for gearshifts which occur after sufficiently long fixed-gear phases of the transmission system, as torque converters are designed to attain the coupling mode quickly in order to avoid high drag losses. It should also be noted that the different modes of a torque converter can be determined from the velocities of the turbine and pump shafts, more specifically their ratio. Since these velocities are measured variables, information regarding the operating mode of the torque converter is always known. However, the dependence of the mode of the torque converter on the speed ratio of the turbine and pump shafts might change with operating conditions. If so, this dependency should be incorporated in the controller design. Under the assumption of locked torque converter clutch or fluid coupling mode, (1) is modified to,

$$\dot{\omega}_e = \frac{1}{I_e}[T_i(\omega_e, \alpha) - T_t - T_f - b_e\omega_e]. \tag{20}$$

It is further assumed that T_i, T_f, and b_e are known. Information on T_f, b_e is known through initial engine calibration, and engine indicated torque T_i is estimated online, and usually found on the CAN bus of a vehicle. Due to the fact that it is estimated in real time, perhaps by using a reduced-order engine model, the information on the indicated torque is not exact, which is why it will be considered as one of the uncertain quantities for validating robustness of the controller in Section 5.

A sliding mode observer (Utkin, Guldner, & Shi, 2009) is proposed for the estimation of turbine torque during the torque phase,

$$\begin{aligned} \dot{\hat{\omega}}_e &= \frac{1}{I_e}[-b_e\hat{\omega}_e + v_1] \\ v_1 &= k_1 \text{sign}(\omega_e - \hat{\omega}_e), \quad k_1 > 0 \end{aligned} \tag{21}$$

which gives the following error dynamics equation

$$\dot{\tilde{\omega}}_e = \frac{1}{I_e}[-b_e\tilde{\omega}_e + T_i - T_t - T_f - v_1]. \tag{22}$$

Now if $k_1 > |T_i| + |T_t| + |T_f|$, then the estimation error $\tilde{\omega}_e$ converges asymptotically to zero. Upper bounds on T_i, T_f, and T_t are usually known which can be used to select the gain k_1. Note that finite time convergence of $\tilde{\omega}_e$ to zero can be achieved if $k_1 > |T_i|+|T_t|+|T_f|+|b_e\tilde{\omega}_e|$ or $k_1 > |T_i| + |T_t| + |T_f| + |b_e\tilde{\omega}_e(0)|$, where $\tilde{\omega}_e(0)$ is the initial estimation error that can be made arbitrarily small by choosing the observer's initial condition in (21) to be close to the sensed value of ω_e at that initial time instant. This was the methodology adopted for the current study.

Once convergence of the estimation error to zero takes place, the method of equivalent control (Utkin et al., 2009) can be used, which ensures the existence of a (low-frequency) signal $v_{1,eq}$ equivalent to the (high-frequency) signal v_1 such that on the convergence of the estimation error $\tilde{\omega}_e$ to zero, we have

$$v_{1,eq} = T_i - T_t - T_f \tag{23}$$

where $v_{1,eq}$ is the equivalent *control* corresponding to $v_1 = k_1\text{sign}(\tilde{\omega}_e)$ and physically represents its low frequency component. Thus, if $v_{1,eq}$ is known, then by using the previous assumptions of known T_f and T_i, the turbine torque can be calculated. The equivalent control ($v_{1,eq}$) can be extracted from its corresponding high frequency signal v_1 by low-pass filtering it (Utkin et al., 2009). Thus the following low pass filter was designed,

$$\tau_1\dot{v}_{1,f} + v_{1,f} = v_1 \tag{24}$$

where τ_1 is the time constant of the filter and $v_{1,f}$ is the filter output. It was shown in Utkin et al. (2009) that $v_{1,f} \to v_{1,eq}$ if and only if $\tau_1 \to 0$ and $\Delta/\tau_1 \to 0$, where $\Delta \approx 1/f_s$ and f_s is the switching frequency for the term $k_1\text{sign}(\tilde{\omega}_e)$, which in the case of an observer is limited by the time step of the fixed step solver. This necessary and sufficient condition requires that the onboard processor for implementation of the proposed observer should be sufficiently fast to avoid a first order lag between the filter output and the equivalent control. It is proposed that the time constant τ_1 should be tuned to minimize this lag, if the onboard processor is not sufficiently fast.

If the assumption on coupling of the turbine and pump sides of the torque converter at the beginning of the commanded gearshift is violated, the turbine torque observer will be estimating the pump torque as opposed to the turbine torque in the torque amplification mode. Using Kotwicki's model ((2) and (3)) an estimate of this difference can be derived to be,

$$\begin{aligned} \Delta_{T_t} &:= T_t\big|_{TA} - T_p\big|_{TA} \\ &= (b_0 - a_0)\omega_p^2 + (b_1 - a_1)\omega_t\omega_p + (b_2 - a_2)\omega_t^2 \end{aligned} \tag{25}$$

where TA denotes the torque amplification mode. The quantity Δ_{T_t} is positive as, during the torque amplification mode, the turbine torque is always higher than the pump torque. Due to error in the estimation of the turbine torque, the estimation of the load torque at the offgoing clutch, to be described next, will be off by $\alpha_2\Delta_{T_t}$, see (7), where the parameter $\alpha_2 < 0$. Thus the reaction torque will be overestimated, resulting in a potential clutch tie-up. Thus it is necessary to switch the torque phase observer for estimation of the turbine torque from the

one proposed here to the open-loop estimator, which would simply use Kotwicki's model.

We proceed by applying a technique similar to the one above to (6) to estimate the term $\mu(\omega_{sr})P_{c,ND}$ which, along with the estimated turbine and output shaft torques, is used to evaluate the reaction torque at the offgoing clutch (using (7)). Also, under the assumption of known coefficient of friction $\mu(\omega_{sr})$, the oncoming clutch pressure is known. However, any uncertainty in the coefficient of friction will induce corresponding uncertainty in the clutch pressure estimate. Thus the controller will be made robust against this and other estimation errors in Section 4.

3.3. Inertia phase observer design

Due to appreciable changes in the speed of the transmission input shaft during the inertia phase, the torque converter mode may change during this phase of the shift. Thus, a new observer needs to be designed for the estimation of the turbine torque in this phase. The turbine torque and oncoming clutch pressure are simultaneously estimated. One of the control actions during the inertia phase is to completely release the offgoing clutch, thus (8) becomes,

$$\begin{aligned}\dot{\omega}_{sr} &= q_1 T_s + q_2 T_t + q_3 \mu(\omega_{sr}) P_{c,ND} \\ \dot{\omega}_{cr} &= p_1 T_s + p_2 T_t + p_3 \mu(\omega_{sr}) P_{c,ND}.\end{aligned} \tag{26}$$

If the offgoing clutch pressure, and thus the offgoing clutch reaction torque, is not zero at the beginning of the inertia phase, it serves as a disturbance input to the observer designed using (26). The observer is designed using the same principles as for the torque phase sliding mode observer.

$$\begin{aligned}\dot{\hat{\omega}}_{sr} &= \upsilon_2 = k_2 \text{sign}(\tilde{\omega}_{sr}),\ \tau_2 \dot{\upsilon}_{2,f} + \upsilon_{2,f} = \upsilon_2, \\ \dot{\hat{\omega}}_{cr} &= \upsilon_3 = k_3 \text{sign}(\tilde{\omega}_{cr}),\ \tau_3 \dot{\upsilon}_{3,f} + \upsilon_{3,f} = \upsilon_3\end{aligned} \tag{27}$$

where the symbols have the same meanings as defined for the torque phase observer. In particular, $\upsilon_{2,f}$ and $\upsilon_{3,f}$ are estimates of the right hand sides of Eq. (26), respectively. Then using the estimated shaft torque from the Luenberger observer,

$$\begin{bmatrix} \hat{T}_t \\ \mu(\omega_{sr})\hat{P}_{c,ND} \end{bmatrix} = \begin{bmatrix} q_2 & q_3 \\ p_2 & p_3 \end{bmatrix}^{-1} \left(\begin{bmatrix} \upsilon_{2,f} \\ \upsilon_{3,f} \end{bmatrix} - \begin{bmatrix} q_1 \\ p_1 \end{bmatrix} \hat{T}_s \right) \tag{28}$$

where the inverse can be shown to always exist, which is intuitive as the turbine torque and the oncoming clutch pressure serve as independent actuators for the slip speeds. Clearly, as the estimation error of the shaft torque goes to zero, estimation errors of the turbine torque and oncoming clutch pressure go to zero. Again, under the assumption of known $\mu(\omega_{sr})$, the oncoming clutch pressure is known. Based on the information provided by the observer, a controller may be designed for the closed loop control of both the torque and inertia phases.

4. Controller design

Due to differences in the governing differential equations of the transmission system, control design is implemented differently for the torque and inertia phases. However, the basic control philosophy remains the same for both the phases. The structure of the controller is shown in Fig. 7. The controller is composed of two components having a cascaded connection. The feedback linearization controller calculates the clutch pressure trajectory required for desired speed tracking, which in turn serves as a reference input for the sliding mode controller. The key thing to notice is the modularity of the controller structure which effectively reduces the problem of designing a controller for a larger state-space to the problem of designing two controllers for smaller state spaces. The cascaded controllers also have different robustness requirements, which simplifies the design problem in the sense that controller designs appropriate for the different levels of robustness can be used. In the field of sliding mode and nonlinear control, this is known as control design by regular form (Utkin et al., 2009). The methodology of control design by regular form is a natural choice for transmission systems due to the cascaded (serial) structure of the same, where the coupling between the hydraulic and mechanical systems is unidirectional.

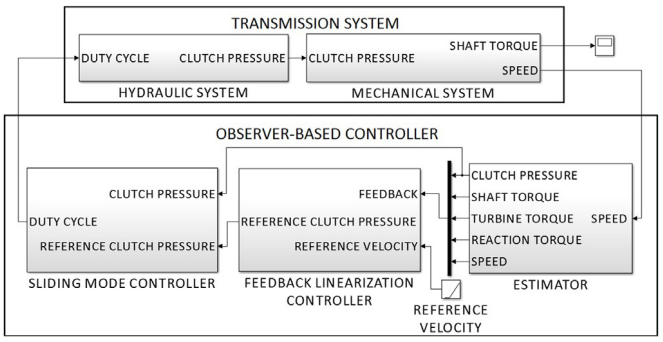

Fig. 7. Cascaded controller architecture.

4.1. Sliding mode control of the transmission shift hydraulic system

The sliding mode controller will be derived for the reduced order shift hydraulic model derived earlier, see (13), where the control input γ takes values in the closed set $[0, 1]$. This is different from the usual case for control inputs in sliding mode control systems, where the control input assumes values symmetric about zero. We design the following linear transformation for the control input γ in order to adhere to the convention.

$$u = 2\gamma - 1. \tag{29}$$

The equations in (13) can be combined and rewritten to incorporate this transformation as,

$$\dot{P}_c = \frac{K_a}{A_a}\left(\frac{f^+ + f^-}{2} + \frac{f^+ - f^-}{2}u\right) \tag{30}$$

where the subscript avg is dropped, as the first order model response was shown to be close to the response of the third order model.

The problem of trajectory tracking can now be formally stated: for a given reference clutch pressure trajectory P_c^*, design a sliding mode controller such that the trajectory tracking error, $\tilde{P}_c := Pc^* - P_c$, converges to zero asymptotically. Sliding mode controllers possess the property of finite time convergence, i.e., the tracking error goes to zero after some finite time, if feedback is available from sensor measurements. However, if the signals involved in the feedback are estimated with the estimates converging asymptotically to exact values, then this attractive property of finite time convergence is lost. In the current study, availability of the oncoming clutch pressure sensor is not assumed, and the required clutch pressure is estimated asymptotically. Consequently, the control problem statement requires only asymptotic convergence of the tracking error to zero.

The following sliding surface (manifold) was designed to solve the stated control problem,

$$s = P_c - P_c^*. \tag{31}$$

The rate of change of this sliding variable was calculated as,

$$\dot{s} = \frac{K_a}{A_a}\left(\frac{f^+ + f^-}{2}\right) + \frac{K_a}{A_a}\left(\frac{f^+ - f^-}{2}\right)u - \dot{P}_c^*. \tag{32}$$

In order to ensure the condition

$$s\dot{s} < 0 \tag{33}$$

for the convergence of the variable s to zero, the following control input u was selected.

$$\begin{aligned} u &= u_{eq} - \epsilon\ \text{sgn}(s) \\ u_{eq} &= \frac{2A_a}{K_a(f^+ - f^-)}\left(-\frac{K_a}{A_a}\left(\frac{f^+ + f^-}{2}\right) + \dot{P}_c^*\right). \end{aligned} \tag{34}$$

The control input has two components: u_{eq} denotes the equivalent control (Utkin et al., 2009) while the second term, $\epsilon\ \text{sgn}(s)$, is added for

robustness. The quantity ϵ can be a constant parameter that needs to be calibrated, or it can be calculated as a function of states using Lyapunov arguments (Shen et al., 2005). In the current study, a constant value of ϵ was found to be adequate. Also, $f^+ > 0,\ f^- < 0$ during a gearshift, which implies that the factor $(f^+ - f^-) \neq 0$, further implying that the control input is well defined during the gearshift.

4.2. Torque phase controller design

The primary goal in torque phase controller design is to prevent any mis-coordination of the offgoing and oncoming clutches resulting in engine tie-up or flare, as both of these situations result in larger torque variation in the output shaft torque response. A secondary goal is to control the duration of the torque phase. The two objectives were met by the following controller. The primary goal of coordinating the two clutches can be achieved by monitoring the estimated reaction torque at the offgoing clutch and designing a controller such that the offgoing clutch behaves like a one-way clutch, i.e., the offgoing clutch transfers torque only in one direction. This further means that the offgoing clutch pressure must be manipulated to maintain a clutch torque capacity which is higher than the estimated offgoing clutch reaction torque for all times during the torque phase and converges to zero with it. Towards this end, the desired torque capacity of the offgoing clutch ($T^*_{c,LR}$) is defined to be a linear function of the (estimated) reaction torque, i.e.

$$T^*_{c,LR} = \epsilon \hat{R}T_{LR}, \quad \epsilon > 1 \tag{35}$$

where ϵ is some constant greater than one. The constant ϵ is a safety factor (cushion) in the face of uncertainty in the estimate of the reaction torque at the offgoing clutch. If some maximum estimate of the estimation error of the reaction torque ($\tilde{R}T_{LR}$) at the offgoing clutch, denoted by $\tilde{R}T_{LR,max}$, is known, then ϵ can be selected to ensure the following at the start of the torque phase,

$$T^*_{c,LR}(t_o) > \hat{R}T_{LR}(t_o) + \tilde{R}T_{LR,max} \tag{36}$$

where t_o denotes the start of the torque phase. This was the methodology adopted in the current work. The desired torque capacity can be converted to the desired clutch pressure of the offgoing clutch using (4).

$$P^*_{c,LR} = \frac{1}{\mu(\omega_{cr})A_{c,LR}R_{c,LR}\mathrm{sgn}(\omega_{cr})}T^*_{c,LR}. \tag{37}$$

For transmissions equipped with the offgoing clutch pressure sensor, this desired clutch pressure trajectory is sent to the sliding mode controller where, by using feedback from the pressure sensor, the problem of clutch pressure trajectory tracking is solved. For transmission systems without any clutch pressure sensors, this needs to be done in an open loop fashion. The only piece of information that is needed is the delay between the command given to the PWM solenoid valve to release the clutch and the actual release of the clutch, which is usually known to a sufficient degree of accuracy. Also, it should be noted that variable force solenoids (VFS) used in newer generation transmission systems have in-built mechanical feedback (Bai, Maguire, & Peng, 2013) due to which the commanded following is accurate, i.e., the clutch pressure is fairly close to the commanded solenoid pressure.

The secondary goal of controlling the duration of the torque phase can be realized in the following manner. Eqs. (6) and (7) can be combined to give,

$$RT_{LR} = \beta_1 T_s + \beta_2 T_t + \beta_3 \dot{\omega}_{sr} \tag{38}$$

where $\beta_1,\ \beta_2,\ \beta_3$ are known constants. Since there are only small speed changes during the torque phase, we assume that $\dot{\omega}_{sr} \approx 0$. Also assuming that the engine indicated torque is not manipulated during the shift, the turbine torque roughly remains constant. Using these arguments (38) becomes,

$$\dot{RT}_{LR} \approx \beta_1 \dot{T}_s \tag{39}$$

which establishes the fact that during the torque phase, the load torque at the offgoing clutch can be controlled by controlling the driveshaft torque T_s, which in turn can be controlled by controlling the speed at the output of the transmission ω_o, see (14), as the vehicle speed ω_v remains approximately constant during the entire gearshift. Thus define

$$\xi := -\frac{\hat{R}T_{LR}(t_o)}{\Delta t_T} \tag{40}$$

where $\hat{R}T_{LR}(t_o)$ denotes the estimated value of the reaction torque at the start of the torque phase and Δt_T is the desired duration of the torque phase. The reference trajectory (ω^*_o) for ω_o is then defined as,

$$\omega^*_o = \omega_v + \frac{\xi}{K_s\beta_1}. \tag{41}$$

Under the assumption that ω_o converges to ω^*_o,

$$\dot{T}_s = \frac{\xi}{\beta_1}. \tag{42}$$

This gives, using (39),

$$\dot{RT}_{LR} \approx \xi. \tag{43}$$

Integrating both sides, we have

$$RT_{LR}(t_o + \Delta t_T) - RT_{LR}(t_o) \approx \xi \Delta t_T. \tag{44}$$

Now, using the definition of ξ and under the assumption that $\hat{R}T_{LR}(t_o) = RT_{LR}(t_o)$,

$$RT_{LR}(t_o + \Delta t_T) \approx 0 \tag{45}$$

which shows that the duration of the torque phase is Δt_T. It should be noted that the quantity $\hat{R}T_{LR}(t_o)$ was not calculated using the torque phase observer described above, but by using a similar observer for the transmission system in the first gear. This is important to understand since the torque phase observer will take some amount of finite time to converge and thus the assumption of $\hat{R}T_{LR}(t_o) = RT_{LR}(t_o)$ will not be valid, no matter how small that time duration is.

It should be noted that during the torque phase the change in the speed of the output shaft of the transmission is small, as will be pointed out in Section 5. Thus a strategy needs to be devised to extract this small change from the (possibly) noisy sensor measurement to be used as feedback for the tracking controller (to be described next), which ensures convergence of ω_o to ω^*_o. In the current study, the disturbance rejection controller (to be described in Section 4.4) is a Kalman filter that uses the noisy tracking error signal $\omega_o - \omega^*_o$ for estimating model errors and external disturbances, also produces a filtered estimate of the tracking error signal, thus eliminating the need for a dedicated filter.

The only other result that remains to be shown is the convergence of ω_o to ω^*_o. During the torque phase, ω_o is kinematically related to the clutch slip speed ω_{sr}. Thus, (6) can be rewritten as

$$\dot{\omega}_o = d_1 T_s + d_2 T_t + d_3 \mu(\omega_{sr}) P_{c,ND} \tag{46}$$

where d_1, d_2, and d_3 are known constants. Using the feedback linearization control technique, the following desired clutch pressure trajectory is proposed

$$P^*_{c,ND} = \frac{1}{d_3\mu(\omega_{sr})}(-d_1\hat{T}_s - d_2\hat{T}_t + \dot{\omega}^*_o - \lambda_T(\omega_o - \omega^*_o)) \tag{47}$$

where λ_T is a positive constant which determines the rate of convergence of the tracking error ($\tilde{\omega}_o := \omega_o - \omega^*_o$) to zero. Under the assumption that the estimation errors of T_s and T_t converge to zero sufficiently fast, we have (from (46), (47))

$$\dot{\tilde{\omega}}_o = -\lambda_T \tilde{\omega}_o \tag{48}$$

which clearly shows that $\tilde{\omega}_o \to 0$ asymptotically. Again, clutch pressure trajectory tracking for the oncoming clutch is achieved through the sliding mode controller described earlier in this subsection and would use the estimated value of the oncoming clutch pressure ($\hat{P}_{c,ND}$) as feedback for transmission systems with no clutch pressure sensor.

4.3. Inertia phase controller design

The inertia phase controller should be designed to ensure a short inertia phase duration and smooth clutch slip speed change. A short inertia phase duration implies longevity of the friction elements (friction clutches and band brakes) of the transmission system, albeit at the potential expense of shift *smoothness*. The two objectives are conflicting in nature and thus the design of the reference clutch slip speed is critically important. Due to the lack of formal approaches for the selection of such a reference, we select the reference trajectory using simpler physical reasoning. The following reference clutch slip speed trajectory (ω^*_{sr}) is selected in the current study (Gao et al., 2012).

$$\omega^*_{sr}(t) = \frac{2\omega_{sr}(t_i)}{(t_f - t_i)^3}(t - t_i)^3 - \frac{3\omega_{sr}(t_i)}{(t_f - t_i)^2}(t - t_i)^2 + \omega_{sr}(t_i) \tag{49}$$

where t_i, t_f represent the start and end times of the inertia phase, $t \in [t_i, t_f]$, and $\omega_{sr}(t_i)$ denotes the sensed slip speed of the oncoming clutch at the start of the inertia phase.

A few remarks regarding the selected reference trajectory are in order. The initial tracking error ($\tilde{\omega}_{sr}(t_i) := \omega_{sr}(t_i) - \omega^*_{sr}(t_i)$) and derivative of the reference trajectory are zero at the start of the inertia phase, which prevents controller saturation at this time instant. Also, the derivative of the desired reference trajectory is zero at the end of the inertia phase which ensures zero shock at clutch lockup with perfect tracking.

The inertia phase controller also uses a combination of feedback linearization and sliding mode controllers to achieve the desired clutch slip trajectory tracking. First, note that, since the offgoing clutch is completely released at the end of the torque phase ideally, the differential equation for the oncoming clutch slip speed during the inertia phase becomes, see (8),

$$\dot{\omega}_{sr} = q_1 T_s + q_2 T_t + q_3 \mu(\omega_{sr}) P_{c,ND}. \tag{50}$$

Adopting a procedure similar to the one described for the tracking control of final drive output shaft speed ω_o, the following desired oncoming clutch pressure trajectory is proposed.

$$\begin{aligned} P^*_{c,ND} &= \frac{1}{q_3 \mu(\omega_{sr})}(-q_1 \hat{T}_s - q_2 \hat{T}_t + \dot{\omega}^*_{sr} + z) \\ z &= -\lambda_I(\omega_{sr} - \omega^*_{sr}) \end{aligned} \tag{51}$$

where $\lambda_I > 0$ controls the rate of convergence of the tracking error $\tilde{\omega}_{sr}$ to zero, which can be seen from the resulting error dynamics equation.

$$\dot{\tilde{\omega}}_{sr} = -\lambda_I \tilde{\omega}_{sr}. \tag{52}$$

In deriving the above error dynamics, we have assumed that the estimation errors of the turbine and shaft torques converge to zero sufficiently fast.

4.4. Robust feedback linearization controller design

For each phase of the shift, the controller uses a combination of feedback linearization and sliding mode control techniques. It is a widely accepted fact that the sliding mode controller is robust against parametric uncertainties and external disturbances which satisfy the matching condition (Edwards & Spurgeon, 1998). The matching condition implies that the disturbance (and parametric uncertainties, which can be modeled as disturbances) enters the system dynamics through the same channels as the control input, i.e., the disturbance should share the same range space as the control input. On the other hand, the feedback linearization technique requires exact information about the model and its performance degrades with any kind of uncertainty. In the current study, the lumped compliance of the driveline K_s, clutch coefficient of friction μ, information on engine indicated torque T_i, and information on the vehicle load torque T_L are assumed to be uncertain, which give rise to estimation errors. The objective of robust control is to ensure graceful, though not optimal, performance of the controller in the face of these uncertainties.

The incorporation of robustness in the controller will be demonstrated only for the inertia phase, as the process is identical for the torque phase. The error dynamics for the oncoming clutch slip speed tracking for the nominal (without the aforementioned sources of uncertainty) system was derived in (52), which changes to the following if various forms of uncertainty are present in the system.

$$\dot{\tilde{\omega}}_{sr} = -\delta_1 \lambda_I \tilde{\omega}_{sr} + \delta_2 \tag{53}$$

where the multiplicative uncertainty $\delta_1 = 1 + \frac{\Delta\mu}{\mu}$, and $\Delta\mu$ is the uncertainty in the clutch coefficient of friction μ. The additive uncertainty δ_2 is a function of various aforementioned uncertainties, the exact form of which is not critical for the discussion here. As long as the uncertainty in the clutch coefficient of friction satisfies $\Delta\mu > -\mu$, the internal stability of (53) due to change in the coefficient of friction is preserved. In general, the change of coefficient of friction over time is positive, which is to say that the friction can only increase through aging, which ensures that the condition on uncertainty $\Delta\mu$ is satisfied. However due to the absence of a reliable aging model for clutch friction, this is difficult to justify formally. These arguments suggest that it is sufficient to take measures for incorporating robustness in the controller against the additive uncertainty δ_2. Thus, δ_1 will be dropped in (53) for designing the disturbance rejection controller to be described next.

The easiest way to ensure controller performance against δ_2 is by estimating and subsequently canceling it through appropriate clutch pressure manipulation. Towards this end, a Kalman filter with an internal model of the disturbance δ_2 is designed. It is assumed here that δ_2 is a low frequency signal, and thus a constant disturbance model for the same is used. During the inertia phase, the feedback linearization controller renders the nonlinear system into a first order linear system with an additive disturbance (δ_2), given by (53), which serves as the plant for designing a standard Kalman filter. Incorporating the disturbance model, the augmented plant model becomes,

$$\begin{aligned} \begin{bmatrix} \dot{\tilde{\omega}}_{sr} \\ \dot{\hat{\delta}}_2 \end{bmatrix} &= \begin{bmatrix} -\lambda_I & 1 \\ 0 & 0 \end{bmatrix} \begin{bmatrix} \tilde{\omega}_{sr} \\ \hat{\delta}_2 \end{bmatrix} + \begin{bmatrix} 0 \\ 1 \end{bmatrix} w \\ y &= \begin{bmatrix} 1 & 0 \end{bmatrix} \begin{bmatrix} \tilde{\omega}_{sr} \\ \hat{\delta}_2 \end{bmatrix} + v \end{aligned} \tag{54}$$

where w is the process noise, and serves as a tuning parameter, and v is the zero mean Gaussian noise present in the oncoming clutch slip speed sensor measurement, which shows up in feedback of the tracking error $\tilde{\omega}_{sr}$. Thus, in addition to estimating the additive disturbance δ_2, the proposed Kalman filter cleans up the noisy speed error signal $\tilde{\omega}_{sr}$, which will be used as feedback. The gains for the Kalman filter designed for the augmented model (54) were calculated using the MATLAB routine *lqe*, which solves an algebraic Riccati equation.

The information on the estimated disturbance $\hat{\delta}_2$ was incorporated in the inertia phase feedback linearization control law as follows.

$$\begin{aligned} P^*_{c,ND} &= \frac{1}{q_3 \mu(\omega_{sr})}(-q_1 \hat{T}_s - q_2 \hat{T}_t + \dot{\omega}^*_{sr} + z - \hat{\delta}_2) \\ z &= -\lambda_I(\omega_{sr} - \omega^*_{sr}). \end{aligned} \tag{55}$$

Application of (55) leads to the following oncoming clutch slip speed tracking error dynamics.

$$\dot{\tilde{\omega}}_{sr} = -\delta_1 \lambda_I \tilde{\omega}_{sr} + \delta_2 - \delta_1 \hat{\delta}_2. \tag{56}$$

So, if the uncertainty in the coefficient of friction is small as compared to its nominal value, i.e. $\delta_1 \approx 1$, the proposed disturbance rejection controller will work once the estimate of the disturbance $\hat{\delta}_2$ converges to δ_2. In case the uncertainty in the clutch coefficient of friction is large, the tracking error does not go to zero asymptotically but is subject to a persistent excitation input. A similar procedure was adopted for ensuring robustness of the torque phase controller, which is not discussed here for the sake of brevity. As described in the section on torque phase control, the Kalman filter for the torque phase, in addition to estimating the model errors, also extracts the small change in the speeds of the transmission output shafts from the noisy measurement signal.

5. Results and discussion

The observer-based controller proposed in the preceding section has been validated on the MATLAB/SIMULINK powertrain model described in Section 2, which represents a production planetary automatic transmission system. We note that while the engine and transmission mechanical simulations use the relatively simple but well accepted models presented here, the simulation of the transmission hydraulic system is particularly detailed, including as it does a third order nonlinear model for each clutch, and large portions of it have been experimentally validated in an earlier work (Watechagit & Srinivasan, 2003), Fig. 6 being one instance of such validation. A fixed step solver with an integration time step of 0.0001 s was used for the simulation. The shift schedule is simplified and solely based on the vehicle speed. As mentioned previously, the power-on 1–2 upshift is a clutch-to-clutch shift, with LR and ND clutches serving roles of the offgoing and oncoming clutches respectively, and is initiated when the vehicle speed is greater than a specified threshold, the threshold being 18.5 km/h. The throttle opening is maintained constant at 10% of wide open throttle for all the simulation results here except for those in Section 5.3. Engine torque management is not explored in the current work. Clutch filling transients are also not included in the simulation. Once the shift is commanded, the simulation goes into the torque phase, where the oncoming clutch pressure is manipulated to drive the load torque at the offgoing clutch to zero in a controlled manner. During this phase, the offgoing clutch is controlled to emulate a one-way clutch. The offgoing clutch torque capacity is manipulated closed-loop under the assumption that the offgoing clutch pressure sensor is available, as is the case for dual clutch transmissions (DCT). Once the torque capacity of the offgoing clutch is lowered to equal the torque carried by the same, it starts slipping and the simulation goes into the inertia phase. During the inertia phase, the offgoing clutch is fully disengaged ideally, and the oncoming clutch pressure is manipulated to drive the oncoming clutch to smooth engagement. Towards the end of the inertia phase, when the slip speed of the oncoming clutch is very small, the threshold being 0.05 rad/s, the feedback linearization controller is deactivated and the clutch pressure is ramped up in an open loop fashion to ensure proper lock-up. In both phases, the feedback linearization controller corresponding to the phase provides the reference pressure trajectory for the sliding mode controller.

5.1. Baseline performance of the controller

We first present simulation results corresponding to the case where the model representation of the transmission system used for the observer-based controller design is the same as one used in the plant except for the hydraulic model, as the controller uses the first-order state-space averaged model of the hydraulic system derived in Section 2.5, whereas the plant includes the third order nonlinear model. This will be referred to as the baseline case. As mentioned earlier, small speed changes during the torque phase may present a challenge for the proposed observer-based controller in the face of appreciable sensor noise, as it relies on speed tracking of the transmission output shaft speed. In order to simulate sensor noise and understand its effect on the controller performance, a zero mean Gaussian noise of variance 1 rad/s was added to the transmission output shaft speed signal ω_o, which serves as the feedback for the torque phase controller. Noise of same magnitude and type was also added to the transmission input shaft speed signal, as the same noise factors are at work for all types of speed sensors in practice. It should be noted that the offgoing and oncoming clutch slip speed signals employed for feedback are derived from the transmission input and output shaft speed signals and thus will reflect the noise characteristics of these signals.

Figs. 8 through 13 show simulation results for the baseline case with added sensor noise, and desired torque and inertia phase time durations of 0.2 s and 0.5 s respectively. The flag variable in Fig. 10, which marks

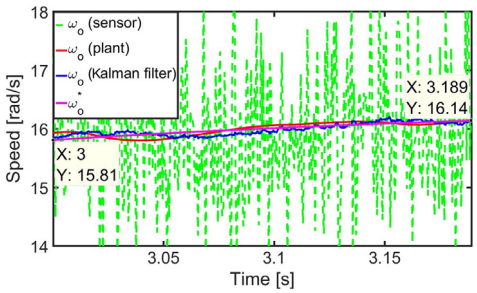

Fig. 8. Transmission output shaft speed tracking performance and signal estimation from the noisy measurement in the torque phase.

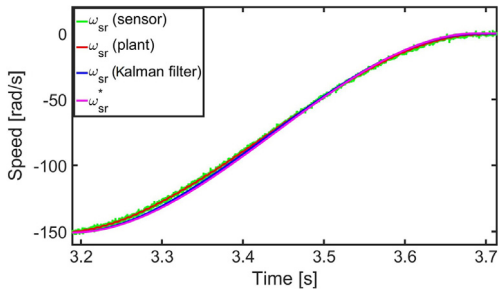

Fig. 9. Oncoming clutch slip speed tracking performance and signal estimation from the noisy measurement in the inertia phase.

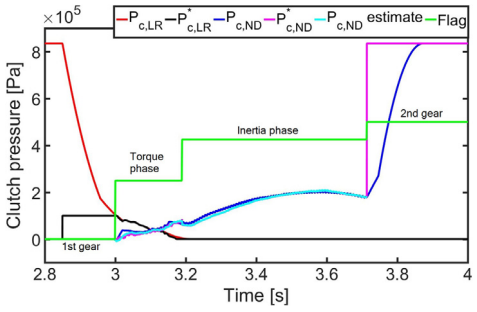

Fig. 10. Clutch pressure tracking performance and oncoming clutch pressure estimation.

the transition of the transmission system through the first gear, torque phase, inertia phase, and second gear, verifies that the actual torque and inertia phase durations are close to their desired values. It can be seen from Fig. 8 that the sensor noise is appreciable as compared to the small change in the output shaft speed reference ω_o^*, where this change is defined as the difference between the initial and final values of ω_o^*, which is equal to 0.33 rad/s. The efficiency of the Kalman filter in estimating the feedback signal from the noisy measurement can also be noted. The tracking performance of the controller during the torque phase is also shown in the same figure, where the speed ω_o remains close to the reference ω_o^*, which leads to the desired torque phase duration. It should be noted that the actual torque phase duration will be longer (shorter) than desired if the net tracking error is negative (positive). In Fig. 9, the Kalman filter is again found to be satisfactory in estimating the speed signal ω_{sr} from noisy sensor measurements. However, in the inertia phase the net change in the reference speed, equal to 150 rad/s, is much larger than the sensor noise. Therefore, after a very short initial transient, the oncoming clutch slip speed tracking can be seen to be accurate.

The fairly accurate speed tracking demonstrated in Figs. 8 and 9 can be attributed to good clutch pressure tracking control achieved by the sliding mode controller, as can be seen from Fig. 10.

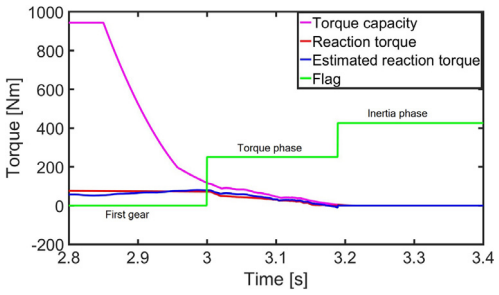

Fig. 11. Offgoing clutch torque capacity manipulation and reaction torque estimation.

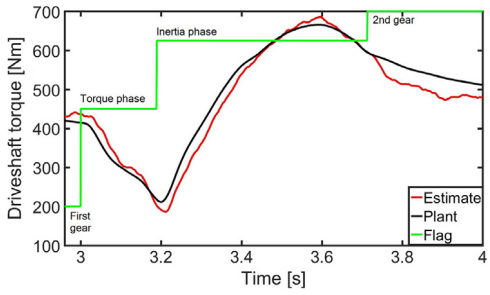

Fig. 12. Driveshaft torque response under the proposed observer-based controller, and its estimation.

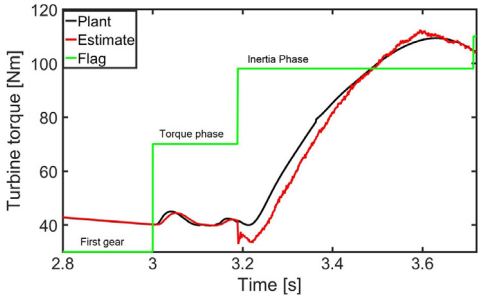

Fig. 13. Turbine torque estimation.

It should also be noted that the reference offgoing clutch pressure $P^*_{c,LR}$ is stepped up well before the initiation of the gearshift, at 2.85 s to be precise. This is done to accommodate the specification on the desired torque phase duration, which happens to be shorter than the *release time* of the offgoing clutch, where the term release time is defined as the delay between the commanded and the actual clutch release. The release time for the offgoing clutch was found to be 0.25 s, implying that it will take more than 0.25 s to disengage the offgoing clutch in a controlled manner. Also, it should be noted that the reference oncoming clutch pressure $P^*_{c,ND}$ is stepped up in an open loop fashion towards the end of the inertia phase to ensure complete engagement, as was mentioned previously.

Fig. 10 also shows accurate estimation of the oncoming clutch pressure $P_{c,ND}$ during both the torque and inertia phases, the performance being better in the inertia phase. This is due to the fact that during the torque phase, estimation error of the oncoming clutch pressure depends on the estimation errors of both the turbine and the driveshaft torques, where as in the inertia phase the oncoming clutch pressure and the turbine torque are simultaneously estimated and their estimation errors depend only on the driveshaft torque estimation error, which from Fig. 12 can be seen to be small. Fig. 11 shows good one-way clutch emulation by the offgoing clutch, where the torque is mainly carried in one (positive) direction. At the end of the torque phase, the torque carried by the offgoing clutch in the negative direction is equal to −11.6 Nm indicating a very minor clutch tie-up. This is due to controlled manipulation of the offgoing clutch torque capacity, which remains higher than the reaction torque and converges to zero with it.

Fig. 12 shows the driveshaft torque response and its estimation under the proposed closed-loop control of clutch-to-clutch shifts. The torque hole and hump, as described in the section on introduction, can be clearly seen, and cannot be eliminated if transmission variables alone are manipulated by the controller. The peak value of the vehicle jerk, occurring at the end of the torque phase, is 2.3×10^{-3} rad/s^3, which indicates acceptable shift quality.

The figure also shows good performance of the driveshaft torque observer. Differences between the actual and estimated driveshaft torque are due to the noise present in feedback of the output shaft speed sensor, as can be seen from Fig. 8, and the wheel speed sensor (signal not shown here), which had to be low-pass filtered before being input to the Luenberger observer for the driveshaft torque. The cut-off frequency used for the low pass filter was 20 Hz.

The estimator performance for turbine torque estimation during the torque and inertia phases is shown in Fig. 13. The estimate of the turbine torque $\hat{T}_t$ can be seen to be close to the actual value of the turbine torque T_t, the reason for the good estimation being related to the torque converter mode during the torque phase. From simulation results for the baseline case, the assumption on coupling of the pump and turbine sides of the torque converter before the start of the shift was found to be valid, as can be seen from Fig. 14. Also as was hypothesized earlier, we see that the torque converter mode of operation remains unchanged during the torque phase, and changes from the fluid coupling to the torque amplification mode during the inertia phase due to large speed changes. We again emphasize that the assumption on coupling is likely to hold whenever a gearshift is initiated after a sufficiently long fixed gear phase of the transmission system. However, if gearshifts are performed with higher frequency, this assumption might not hold, and the turbine torque estimation then should be achieved open-loop using Kotwicki's model or other equivalent model of the torque converter. Doing so, however, would introduce more uncertainty in estimation of turbine torque and deteriorate controller performance.

5.2. Robust performance of the controller

In order to understand the extent of performance deterioration of the proposed observer-based controller in the presence of estimation and modeling errors, errors were introduced in the plant model used by the estimator and controller. More precisely, 30% error was introduced in the lumped driveline compliance K_s, 20% error was introduced in the oncoming clutch friction coefficient $\mu(\omega_{sr})$, 15 Nm error (approximately 15%) was introduced in the engine indicated torque T_i, and 5 Nm error (approximately 25%) was introduced in the load torque T_L. As the percent error levels indicate, these are significant errors that are intended to truly evaluate the effectiveness of the controller features designed to enhance its robustness. To demonstrate the need for specific controller features to enhance robustness, two simulations were performed. In the first, the Kalman filter described in Section 4.4, which estimates model errors as additive disturbances and subsequently cancels their effect by appropriate oncoming clutch pressure manipulation, was deactivated during the inertia phase. In the second simulation, the Kalman filter was active to ensure robust performance of the controller. Figs. 15 and 16 show comparisons between these two simulations, whereas Figs. 17 through 20 show results from the second simulation, in addition to those shown in Figs. 15 and 16.

Fig. 15 shows comparison of the driveshaft torque responses for the cases with and without the inertia phase disturbance rejection controller. Results for the case without the inertia phase disturbance rejection controller can be seen to have a shorter inertia phase due to a higher clutch friction coefficient than that modeled, which results in

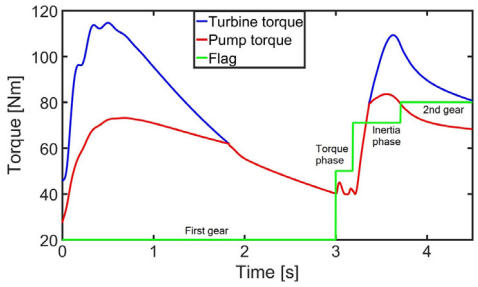

Fig. 14. Pump and turbine torques before, after, and during the 1–2 upshift.

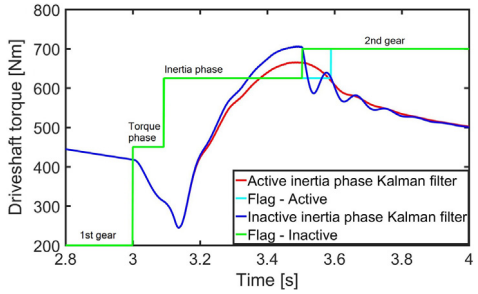

Fig. 15. Driveshaft torque response: with and without the inertia phase Kalman filter.

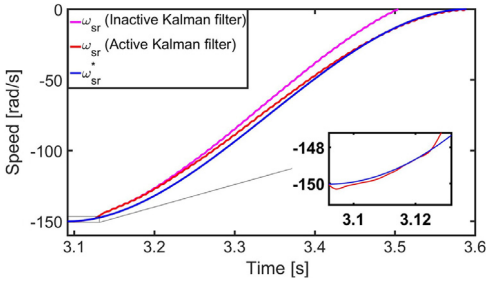

Fig. 16. Oncoming clutch slip speed tracking: with and without the inertia phase Kalman filter.

higher driveshaft torque at lock-up and larger magnitude of oscillation in second gear and a clearly unacceptable shift quality.

The difference in the shift quality for the two cases is due to the differences in oncoming clutch slip speed tracking, which can be seen from Fig. 16. The deceleration of the oncoming clutch for the inactive Kalman filter case remains higher than for the active Kalman filter case throughout the inertia phase due to higher oncoming clutch torque capacity for the former case, which in turn results from the 20% increase in the oncoming clutch friction coefficient in the plant (see (4)) as compared to the model used by the controller. The Kalman filter estimates this model error and nullifies its effect by appropriate oncoming clutch pressure manipulation for the active Kalman filter case, thus resulting in lower levels of deceleration and better shift quality. For both of these simulations, the torque phase controller is kept the same, and includes features to enhance robustness, so that the overall driveshaft torque response for the two simulations are close enough for a fair comparison. The results indicate that model errors introduced in the simulation lead to estimation error and deteriorated controller performance in the absence of the inertia phase disturbance rejection controller.

Error in the lumped driveline compliance and the vehicle load torque induce error in the estimation of the driveshaft torque (not shown here). Error in the indicated engine torque induces commensurate error in the estimate of turbine torque during the torque phase (Fig. 17) which, along with the estimation error of driveshaft torque and model error in the oncoming clutch friction coefficient, induces error in the estimate of oncoming clutch pressure during the torque phase, as can be seen from Fig. 18. During the inertia phase, turbine torque and oncoming clutch pressure are simultaneously estimated and their respective estimation errors result from error in the oncoming clutch coefficient of friction and the driveshaft torque estimation error. Fig. 18 also shows tracking performance of the sliding mode controller which, for the simulation under discussion, uses an estimate of the oncoming clutch pressure but assumes availability of the offgoing clutch pressure signal. The true contribution of the sliding mode controller performance to overall controller effectiveness depends on accuracy of the estimate of the oncoming clutch pressure. We note that the oncoming clutch pressure estimate tracks the reference perfectly, but the actual clutch pressure does not do so.

Errors in estimates of the driveshaft torque, turbine torque, and oncoming clutch pressure induce error in the estimate of the reaction torque at the offgoing clutch, which can be seen from Fig. 19. Due to this error, the offgoing clutch is released early, and carries a non-zero load of approximately 36 Nm at the point when it starts to slip. This non-zero torque carried by the offgoing clutch acts as a disturbance for the inertia phase controller, as the controller was derived under the assumption that the reaction torque at the offgoing clutch is zero at the start of the inertia phase. This disturbance is estimated by the inertia phase Kalman filter and is reflected in step increase of the reference oncoming clutch pressure trajectory at the start of the inertia phase (see Fig. 18, the reference oncoming clutch pressure is hidden by the estimate of the oncoming clutch pressure). It can be seen from Fig. 18 that the reference oncoming clutch pressure is not tracked accurately at the start of the inertia phase due to estimation error of the oncoming clutch pressure, resulting in lower than desired oncoming clutch pressure. This in turn results in further acceleration of the oncoming clutch in the negative direction, see the zoomed-out section in Fig. 16. As the oncoming clutch pressure increases sufficiently, it results in deceleration of the oncoming clutch and in due time in clutch lock-up. Due to the kinematic constraint between the oncoming and offgoing clutch slip speeds for a nearly constant transmission output speed the offgoing clutch slips in the negative direction, as shown in the zoomed-out section in Fig. 20. As the oncoming clutch pressure tracking improves, the oncoming clutch decelerates towards lock-up, resulting in positive slip of the offgoing clutch. Based on the discussion presented in this section, one can note that the controller ensures graceful gearshift response in the face of estimation errors and modeling uncertainties, which indicates a good level of robustness of the proposed observer-based controller.

5.3. *Controller performance at different power levels and for downshifts*

The real utility of the nonlinear estimation and control technique proposed here depends on the performance of the resulting observer-based controller over a wider range of operating conditions and whether re-tuning of controller parameters is needed to ensure good performance. In particular, the ability of the controller to control gearshifts at different power levels is of practical importance. In order to evaluate the effectiveness of the proposed observer-based controller over a wider range of operating conditions, three simulations with different throttle angles were performed, 10%, 15%, and 20% of wide open throttle being the respective values. For all three simulations, the power-on 1–2 upshift was initiated when the vehicle velocity reached a certain threshold. The speed threshold is held the same for all three simulations here, though in practical shift schedules the speed threshold would change with throttle opening. Fig. 21 presents the results corresponding to the three simulations, and shows the driveshaft torque when the proposed closed-loop control strategy is applied, without any change or re-tuning, for the three cases. It should be noted that the driveshaft torque responses during the shifts have similar features in all three cases, indicating that the controller performance does not vary dramatically with the power

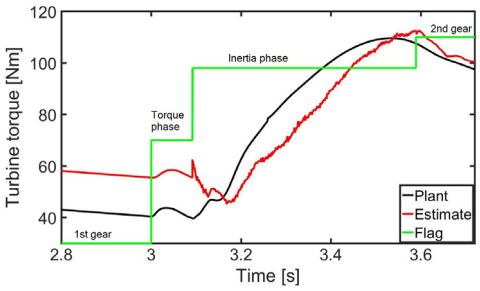

Fig. 17. Turbine torque and its estimate.

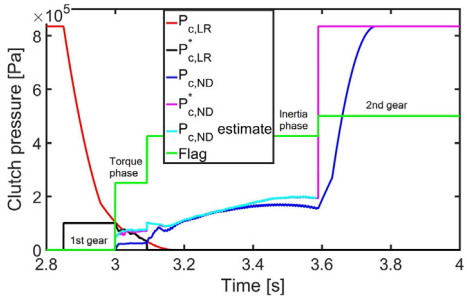

Fig. 18. Clutch pressure tracking performance and oncoming clutch pressure estimation.

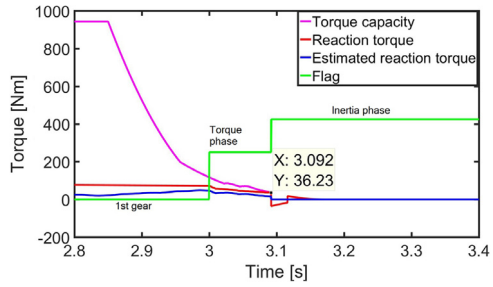

Fig. 19. Offgoing clutch torque capacity manipulation and reaction torque estimation.

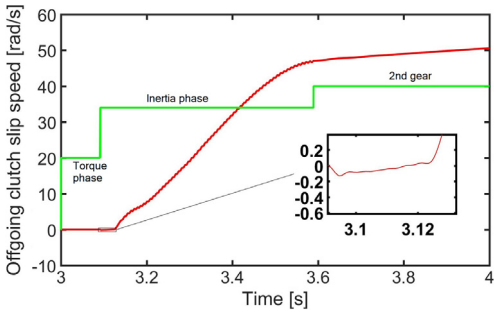

Fig. 20. Offgoing clutch slip speed.

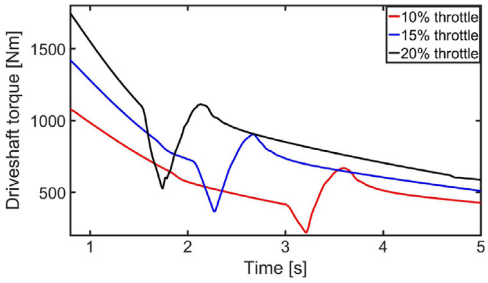

Fig. 21. Driveshaft torque response under the closed-loop control at different throttle openings (power levels).

level at which the gearshift is performed, and that it does not need re-tuning or re-calibration despite the nonlinear nature of the system response. Clearly, the size of the torque hole and hump do vary with the power level. But that is a result of the fact that engine manipulation is not part of the control strategy for the current study, and that only the clutch pressures are manipulated here. Also, for the simulation with 20% throttle opening, at the initiation of the shift, simulation results indicate that the torque converter is operating in the torque amplification mode, whereas for the other two cases, it is in the fluid coupling mode. The controller detects this, and switches to the open-loop estimation of the turbine torque using Kotwicki's model at 20% opening, and yields a satisfactory shift response as indicated by the results. Thus, on-line model-based estimation of the turbine torque enables the quality of the shift to be maintained at a satisfactory level. In the absence of such estimation, the current approach in practice would rely upon calibration of the shift control parameters over a range of throttle openings, with constant control parameters being chosen to ensure a reasonable, albeit lower, level of performance. Further, the cost in additional calibration effort would be significant.

Downshifts occur under wider ranges of operating conditions as compared to upshifts due to which, current practice in controller adjustments for downshifts would involve a much greater level of calibration effort as compared to that incurred in controller adjustments for upshifts. The strategy proposed in the current study for controlling clutch-to-clutch shifts is model-based and incorporates online estimation of various critical operating variables, implying improved knowledge of operating conditions under which downshifts would occur. This naturally would reduce the level of calibration efforts and, further, would improve downshift control performance. The structure of the controller developed here for upshifts will remain the same for controlling downshifts, and validation of the effectiveness of the proposed strategy in controlling downshifts is currently in progress.

6. Conclusions and future work

Tools from nonlinear estimation and control theory have been used here with success, to derive model-based closed-loop control laws for both the torque and the inertia phases of clutch-to-clutch power-on upshifts in automatic transmissions. Extension of model-based closed loop control to the torque phase is a significant contribution of this paper, as is the development of robust model-based control of clutch-to-clutch shifts.

A control-oriented reduced order model of the transmission hydraulic system was derived and validated, based on which a clutch pressure controller was designed. Novel model-based algorithms for online estimation of driveshaft torque, oncoming clutch pressure, turbine torque, and reaction torque at the offgoing clutch using the engine, wheel, and transmission input and output speed sensors were developed and validated using a powertrain simulation including a detailed shift hydraulic system model. It was shown that the reaction torque estimate at the offgoing clutch during the torque phase enables the controller to ensure near one-way clutch operation of the same, thereby ensuring smooth coordination between the offgoing and oncoming clutches. Also, it was shown that the oncoming clutch pressure estimate enables improved oncoming clutch pressure control. Robustness of the proposed controller against appreciable and realistic modeling errors was validated as well. In particular, 20% uncertainty in the clutch coefficient of friction, 30% uncertainty in the lumped driveline compliance, 15% uncertainty in the knowledge of engine indicated torque, and 25% uncertainty in the knowledge of vehicle load torque were introduced

in the model used by the controller. In addition to this, the proposed observer-based controller was shown to be effective in controlling gearshifts at different power-levels, which demonstrates satisfactory controller performance over a range of operating conditions without re-tuning of the controller. This also suggests, importantly, that the proposed controller will be effective in controlling downshifts, which are known to occur over a wider range of operating conditions and usually need higher levels of calibration effort when (non model-based) controllers are used for shift control.

We propose, and are currently involved in, the following extensions of the current work. First, the control philosophy adopted in the current study should be extended to include engine variables, in order to eliminate the torque hole and hump in the output shaft torque response and thus achieve an integrated powertrain control structure. Second, the proposed controller should be extended to cover a wider range of clutch-to-clutch shifts, namely, power-on down shifts, and power-off up-shifts and down shifts. Third, incorporation of estimation and control actions in the clutch fill phase within the overall control strategy for clutch-to-clutch shifts is essential for practical utility of this strategy. Finally, experimental validation of the strategy on current generation powertrains and its impact on transmission calibration efforts will be evaluated.

Acknowledgments

The authors thank the reviewers for their insightful comments that helped the authors identify more clearly the contributions of this work, as well as to highlight relevant issues that continue to be significant.

References

Azzoni, P., Moro, D., Ponti, F., & Rizzoni, G. (1998). *Engine and load torque estimation with application to electronic throttle control. SAE technical paper 980795*.

Bai, S., Brennan, D., Dusenberry, D., Tao, T., & Zhang, Z. (2010). *Integrated powertrain control. SAE technical paper 2010-01-0368*.

Bai, S., Maguire, J. M., & Peng, H. (2013). *Analysis and control system design of automatic transmissions*. SAE International.

Barr, M. P. (2014). *Dynamic modeling, friction parameter estimation, and control of a dual clutch transmission* Ohio State University.

Cho, D., & Hedrick, J. K. (1989). Automotive powertrain modeling for control. *Journal of Dynamic Systems, Measurement, and Control*, *17*(3), 534–546.

Crowther, A., Zhang, N., Liu, D., & Jeyakumaran, J. (2004). Analysis and simulation of clutch engagement judder and stick-slip in automotive powertrain systems. *Proceedings of the Institution of Mechanical Engineers, Part D: Journal of Automobile Engineering*, *218*(12), 1427–1446.

Edwards, C., & Spurgeon, S. (1998). *Sliding mode control: Theory and applications*. CRC Press.

Gao, B., Chen, H., Hu, Y., & Sanada, K. (2011). Nonlinear feedforward–feedback control of clutch-to-clutch shift technique. *Vehicle System Dynamics*, *49*(12), 1895–1911.

Gao, B., Chen, H., Li, J., Tian, L., & Sanada, K. (2012). Observer-based feedback control during torque phase of clutch-to-clutch shift process. *International Journal of Vehicle Design*, *58*(1), 93–108.

Gao, B., Chen, H., & Sanada, K. (2008). Two-degree-of-freedom controller design for clutch slip control of automatic transmission. *SAE technical paper 2008-01-0537*.

Gao, B. Z., Chen, H., Sanada, K., & Hu, Y. (2011). Design of clutch-slip controller for automatic transmission using backstepping. *IEEE/ASME Transactions on Mechatronics*, *16*(3), 498–508.

Goetz, M., Levesley, M., & Crolla, D. (2005). Dynamics and control of gearshifts on twin-clutch transmissions. *Proceedings of the Institution of Mechanical Engineers, Part D: Journal of Automobile Engineering*, *219*(8), 951–963.

Hojo, Y., Iwatsuki, K., Oba, H., & lshikawae, K. (1992). Toyota five-speed automatic transmission with application of modern control theory. *SAE technical paper 920610*.

Hu, Y., Tian, L., Gao, B., & Chen, H. (2014). Nonlinear gearshifts control of dual-clutch transmissions during inertia phase. *ISA Transactions*, *53*(4), 1320– 1331 Disturbance Estimation and Mitigation.

Kotwicki, A. (1982). Dynamic models for torque converter equipped vehicles. *SAE technical paper 820393*.

Kulkarni, M., Shim, T., & Zhang, Y. (2007). Shift dynamics and control of dual-clutch transmissions. *Mechanism and Machine Theory*, *42*(2), 168– 182.

Liu, Z., Gao, J., & Zheng, Q. (2011). Robust clutch slip controller design for automatic transmission. *Proceedings of the Institution of Mechanical Engineers, Part D: Journal of Automobile Engineering*, *225*(8), 989–1005.

Louca, L. S., Stein, J. L., Hulbert, G., & Sprague, J. (1997). Proper model generation : An energy based methodology. *Simulation Series*, *29*, 44–49.

Mishra, K. D., & Srinivasan, K. (2015). Robust nonlinear control of inertia phase in clutch-to-clutch shifts. *IFAC-PapersOnLine*, (ISSN: 2405-8963) *48*(15), 277–284.

Mishra, K. D., & Srinivasan, K. (2016). Robust nonlinear estimation and control of clutch-to-clutch shifts. In *2016 American Control Conference* (pp. 7555–7560.

Pavkovi, D., Deur, J., Kolmanovsky, I., & Hrovat, D. (2008). Application of adaptive kalman filter for estimation of power train variables. *SAE technical paper 2008-01-0585*.

Sanada, K., Gao, B., Kado, N., Takamatsu, H., & Toriya, K. (2012). Design of a robust controller for shift control of an automatic transmission. *Proceedings of the Institution of Mechanical Engineers, Part D: Journal of Automobile Engineering*, *226*(12), 1577–1584.

Sanada, K., & Kitagawa, A. (1998). A study of two-degree-of-freedom control of rotating speed in an automatic transmission, considering modeling errors of a hydraulic system. *Control Engineering Practice*, *6*(9), 1125– 1132.

Shen, X., Zhang, J., Barth, E. J., & Goldfarb, M. (2005). Nonlinear model-based control of pulse width modulated pneumatic servo systems. *Journal of Dynamic Systems, Measurement, and Control*, *128*(3), 563–669.

Utkin, V., Guldner, J., & Shi, J. (2009). *Sliding mode control in electro-mechanical systems*. CRC press.

Vahidi, A., Stefanopoulou, A., & Peng, H. (2005). Recursive least squares with forgetting for online estimation of vehicle mass and road grade: theory and experiments. *Vehicle System Dynamics*, *43*(1), 31–55.

Watechagit, S. (2004). *Modeling and estimation for stepped automatic transmission with clutch-to-clutch shift technology*. Ohio State University.

Watechagit, S., & Srinivasan, K. (2003). Modeling and simulation of a shift hydraulic system for a stepped automatic transmission. *SAE technical paper 2003-01-0314*.

Yoon, A., Khargonekar, P., & Hebbale, K. (1997). Design of computer experiments for open-loop control and robustness analysis of clutch-to-clutch shifts in automatic transmissions. In *Proceedings of the American Control Conference: vol. 5*. (pp. 3359–3364).

Zheng, Q., Srinivasan, K., & Rizzoni, G. (1999). Transmission shift controller design based on a dynamic model of transmission response. *Control Engineering Practice*, *7*(8), 1007–1014.